PRAMANA
— journal of
physics

Vol. 59, No. 4
October 2002
pp. 585–598

Microscopic study of low-lying yrast spectra in $^{100-108}$Mo isotopes

NEERU SAWHNEY, ARUN BHARTI and S K KHOSA
Department of Physics, Jammu University, Jammu 180 006, India

MS received 10 October 2001; revised 16 May 2002

Abstract. Variation-after-projection (VAP) calculations in conjunction with Hartree–Bogoliubov (HB) ansatz have been carried out for $A = 100$–108 molybdenum (Mo) isotopes. In this framework, the yrast spectra with $J^{\pi}_{\max} \geq 10^{+}$, $B(E2)$ transition probabilities, quadrupole (β_2) and hexadecapole (β_4) deformation parameters, moment of inertia (I) and square of cranking frequency (ω^2) for even–even Mo isotopes have been obtained. The results of the calculation give an indication that it is important to include the hexadecapole–hexadecapole component of the two-body interaction for obtaining various nuclear structure quantities in these Mo isotopes.

Keywords. Nuclear structure $^{100-108}$Mo; variation-after-projection calculations; calculated levels; $B(E2)$ transition probabilities; quadrupole (β_2) and hexadecapole (β_4) deformation parameters.

PACS Nos 21.60.-n; 27.60.+J; 21.60.Jz

1. Introduction

The study of nuclei in the mass region $A \approx 100$ has been at the center stage of nuclear physics for quite some time in the past. It all started with an important discovery made by Cheifetz *et al* [1] who discovered a new region of deformation around mass number $A \approx 100$; well developed rotational spectra were observed in several highly neutron-rich isotopes of Zr and Mo during a study of the fission fragments of ^{252}Cf. The observed $B(E2; 0^{+} \rightarrow 2^{+})$ values were as enhanced as in the rare earth and actinide regions. At present we know that the mass region $A \approx 100$, i.e., $38 \leq Z \leq 48$ and $50 \leq N \leq 72$ represents a classic example of dramatic shape changes with particle number [2–7]. In this region, the best examples of shape co-existence are Sr, Zr and Mo isotopes with $N \approx 58$. The Sr and Zr isotopic mass chains show an abrupt transition from spherical to deformed shape at $N = 60$. The transition is smooth for the Mo isotopes and the deformation decreases gradually as Z increases. There is also evidence for the coexistence of spherical and deformed structures in neutron-rich Sr and Zr isotopes.

The occurrence of prolate ground state deformation both in the neutron deficient and neutron rich Zr mass region has provided an important testing ground for various nuclear models and various phenomenological two-body effective nuclear interactions. Some time

back Maharana *et al* [8] have studied the shape coexistence phenomenon in neutron deficient Sr and Zr nuclei in the framework of relativistic mean field approach. Their results on charge radii are found to increase with the removal of neutrons from the semi-magic ^{88}Sr and ^{90}Zr, which is in close agreement with the isotopic shift measurements. Apart from this, Patra and Praharaj [9] also studied the shapes of exotic nuclei in the mass region $A = 70$ using deformed relativistic mean field theory. Their study shows that the ground band deformations for $N = Z$ nuclei are maximum for ^{76}Sr and ^{80}Zr. Now coming to the discussion of neutron-rich nuclei in this mass region, equilibrium deformations and potential energy surfaces in the heavy Zr region were calculated by many authors [6,10–21]. Let us briefly summarize the results of the recent work. The Skyrme–HF model [10] was quite successful in reproducing large deformations around ^{102}Zr. The heavy isotopes of Mo were predicted by this model to be triaxial [13], but experimentally they are found to be axially symmetric [22]. The authors of [10] have noticed the great sensitivity of the model predictions for ^{96,98}Zr to the choice of Skyrme parameters used. For instance, with the SIII set of parameters both ^{96}Zr and ^{100}Zr were predicted to be deformed but experimentally ^{96}Zr is observed to be spherical. On the other hand, results obtained with modified parameters of the Skyrme interaction, SKP, suggested spherical shapes for ^{96,100}Zr. The authors attributed this dramatic change to the variation of neutron single-particle states above the $N = 56$ spherical sub-shell. The shell correction calculations of [16] that were based on the folded-Yukawa average field were quite successful in reproducing experimental masses and large quadrupole deformations in the whole Zr region. However, the transition from a spherical to deformed shape was predicted too early, around $N = 55$. This discrepancy was attributed to insufficient theoretical spherical gaps at $Z = 40$ and $N = 56$. The Nilsson model calculations with standard parameters have also had difficulties in reproducing the suddenness of shape transition. Agreement with experiment was eventually achieved, but only after some modifications of parameters [14,19]. Recently, HB calculations with the surface delta interaction (SDI) was carried out [21] in a rather restricted configuration space (proton shells: $f_{5/2}$, $p_{1/2,3/2}$ and $g_{9/2}$; neutron shells: $s_{1/2}$, $d_{3/2}$, $g_{7/2}$ and $h_{11/2}$). The authors re-emphasized the importance of the *n–p* interaction in relative ^3S states (e.g. interaction between the spin-orbit partners $\pi g_{9/2}$ and $\nu g_{7/2}$).

Completely microscopic calculations in the framework of the density-dependent Hartree–Fock–Bardeen–Cooper–Schrieffer (HF–BCS) approach in conjunction with the Skyrme interaction SVI were carried out by Campi and Epherre [15] for a large number of nuclei with $Z = 36$ and 38. Apart from providing a reasonably successful description of the observed systematics of binding energies and isotope shifts, these mean field self-consistent calculations, which involved an optimized basis of eight major oscillator shells with the constraint of axial symmetry, brought out for the first time the significant role of the inversion of the $2d_{5/2}$ and $1h_{11/2}$ orbits vis-á-vis the observed onset of large deformations at $N = 58$. Bonche *et al* [10] have also reported mean-field calculations of deformation energy surfaces in the region $N = 38$–60 employing the Skyrme interaction SIII. These calculations represented a significant extension of the earlier work by Campi and Epherre [15]. In addition to the inclusion of the triaxial degree of freedom, Bonche *et al* [10] employed discretized configuration space – a feature that obviated the necessity of using the truncated basis. These calculations reproduced the broad features of the observed transition from spherical nuclei to well-deformed rotors and provided significant insight concerning the triaxial softness of the neutron-rich isotopes. The calculations also highlighted the deficiencies of some of the existing versions of the Skyrme interaction; it

was found that neither the interaction SIII nor the interaction SKP could maintain ^{96}Zr as a spherical nucleus while predicting deformation for ^{100}Zr.

From what has been said in the theoretical overview of the work in this region, it is very clear that this region has given an excellent opportunity for testing the validity of various nuclear models and suitability of two-body interactions. In this regard, it was shown by authors in [23–25] that the phenomenological quadrupole–quadrupole plus pairing model of two-body interaction is highly reliable in this mass region. The authors performed Hartree–Bogoliubov (HB) calculation using this effective interaction operating in a valence space spanned by the $2p_{1/2}$, $3s_{1/2}$, $2d_{3/2}$, $2d_{5/2}$, $1g_{7/2}$, $1g_{9/2}$ and $1h_{11/2}$ orbits for protons and neutrons. The parameters of interaction are the right one to be used for this region. The authors demonstrated that the development of the rotational features owes its origin to the significant deformation of $N = 56$ core as well as to the involvement of the $1h_{11/2}$ orbit in the valence space. The latter feature provides an efficient mechanism for increasing deformation since the orbitals $1h_{11/2\pm1/2}$ possess large single particle quadrupole moments. Their calculations concerning the intrinsic deformations, reveal the presence of time reversed $k = \pm 1/2$ neutron–neutron pairs from the $1h_{11/2}$ shell just below the relevant Fermi surfaces in the HB states of $^{100-104}$Mo nuclei. The evidence of occurrence of low-k components of $h_{11/2}$ orbits has been experimentally confirmed in ^{100}Mo by Regan *et al* [26] using deep inelastic reactions. This experimental confirmation of the presence of $(h_{11/2})_\nu$ orbit at the Fermi surface in isotopes with $N \geq 60$ does give the stamp of validity to chosen parameters of the quadrupole–quadrupole plus pairing part of the two-body interaction. However, when the authors attempted a calculation of the low-lying yrast spectra with $J^\pi \leq 8^+$ as well as $B(E2)$ values in the isotopes $^{100-106}$Mo, poor agreement with the observed values was obtained. This, therefore, showed that there is a need for improving upon quadrupole–quadrupole plus pairing model of interaction so that a reasonably good agreement with the experiments can be achieved. This has, therefore, been a motivation for carrying out the present piece of work.

The purpose of the present work is to know whether quadrupole–quadrupole plus pairing model of interaction can further be modified to produce better results in agreement with the experiments. It may be noted that there are many calculations that reproduce the shape transition in the mass region $A \approx 100$ around $N = 60$ but there are very few calculations that have also tried to carry out a spectroscopy of the deformed neutron-rich $N > 60$ nuclei in the same framework and with the same interaction in this mass region. It has become necessary to do so in view of the availability of more useful data on the energy values of new states, e.g., the nuclear spectra in ^{100}Mo is at present known up to 14^+ [26] and now experimentally back-bending is observed in this nucleus at 10^+. Besides this, the yrast spectra for ^{108}Mo has also been obtained [22].

We have examined the available yrast spectra in deformed neutron-rich Mo isotopes with $A > 98$ in the framework of variation-after-projection (VAP) technique in conjunction with the HB ansatz for the trial wavefunctions resulting from the pairing plus quadrupole–quadrupole plus octupole–octupole plus hexadecapole–hexadecapole (VQPOH) whereas the HB form of the trial wavefunction permits a consistent treatment of the pairing and deformation producing components of the effective interaction. The VAP prescription selects an optimum intrinsic state for each yrast levels through a minimization of the expectation value of the Hamiltonian with respect to the states characterized by a definite angular momentum.

Our VAP calculations performed with VQPOH model of two-body interaction shows a marked improvement in agreement with the experimentally observed yrast spectra as compared to the yrast spectra obtained with the VQP interaction. Now, the observed backbending is reproduced in both ^{100}Mo and ^{102}Mo. When only VQP is employed, backbending gets reproduced only in ^{102}Mo. The results obtained for $B(E2)$ transition probabilities and quadrupole deformation (β_2) are found to be in reasonably good agreement with the experiments. The reliability of hexadecapole parameters has also been checked by comparing the values of hexadecapole deformation parameter (β_4) with the values predicted by Möller *et al* [27]. The values of (β_4) obtained with VQPOH are in satisfactory agreement with the values calculated by Möller *et al* [27] for $^{100-104}$Mo.

2. Calculational details

2.1 *The one- and two-body parts of Hamiltonian*

The valence space and the set of spherical single particle energies (SPE's) employed here are exactly the same as used by Sharma *et al* [23] in the zirconium region. The two-body effective interaction that has been employed is of pairing plus quadrupole–quadrupole plus octupole–octupole plus hexadecapole–hexadecapole (VQPOH) type. The parameters of pairing plus quadrupole–quadrupole (VQP) part of the two-body interaction are also the same as used by Sharma *et al* [23]. The relative magnitudes of the parameters of the octupole–octupole and hexadecapole–hexadecapole parts of the two-body interaction were calculated from a relation suggested by Bohr and Mottelson [28]. According to them the approximate magnitude of these coupling constants for isospin $T = 0$ is given by

$$\chi_\lambda = \frac{4\pi}{2\lambda+1}\frac{m\omega_0^2}{A\langle r^{2\lambda-2}\rangle} \quad \text{for} \quad \lambda = 1,2,3,4 \tag{1}$$

and the parameters for the $T = 1$ case are approximately half the magnitude of their $T = 0$ counterparts. This relation was used to calculate the values of χ_{pp3} and χ_{pp4} relative to χ_{pp} by generating the wavefunction for ^{102}Mo and then calculating the values of $\langle r^{2\lambda-2}\rangle$ for $\lambda = 2, 3$ and 4.

The values of these parameters for octupole–octupole interaction work out to be

$$\chi_{\text{pp3}}(=\chi_{\text{nn3}}) = -0.00366\ \text{MeV}\ b^{-6} \quad \text{and} \quad \chi_{\text{pn3}} = -0.00690\ \text{MeV}\ b^{-6}$$

whereas their values for hexadecapole–hexadecapole part of the two-body interaction turn out to be

$$\chi_{\text{pp4}}(=\chi_{\text{nn4}}) = -0.000324\ \text{MeV}\ b^{-8} \quad \text{and} \quad \chi_{\text{pn4}} = -0.000638\ \text{MeV}\ b^{-8}.$$

The procedure for obtaining the axially symmetric Hartree–Bogoliubov (HB) intrinsic states has been discussed in [29]. The methods developed by Onishi and Yoshida [30] for carrying out projection of the states of good angular momentum from axially symmetric HB intrinsic states has been used for obtaining the spectra. The variation-after-projection (VAP) calculations has been carried out as follows: We first generated the self-consistent HB solutions, $\Phi(\beta)$, by carrying out the HB calculations with the Hamiltonian $(H - \beta Q_0^2)$,

where β is a parameter. The selection of the optimum intrinsic states, $\Phi_{\rm opt}(\beta_J)$, is then made by finding out the minimum of the projected energy

$$E_J(\beta) = \langle\Phi_0(\beta)|HP^J_{00}|\langle\Phi_0(\beta)\rangle / \langle\Phi_0(\beta)|P^J_{00}|\Phi_0(\beta)\rangle \tag{2}$$

as a function of β. In other words, the optimum intrinsic state for each yrast J satisfies the conditions

$$\partial/\partial\beta[\langle\Phi_0(\beta)|HP^J_{00}|\Phi_0(\beta)\rangle / \langle\Phi_0(\beta)|P^J_{00}|\Phi_0(\beta)\rangle]|_{\beta=\beta_J} = 0. \tag{3}$$

3. Deformation trends in $^{100-110}$Mo

In table 1, the experimental values of excitation energy of E_2^+ state and intrinsic quadrupole moments of the HB states obtained with the interactions of VQP and VQPOH in the $^{100-110}$Mo isotopes are presented. At this point, we want to make it clear that the addition of octupole–octupole interaction term to the VQPOH interaction does not make any perceivable change in the calculated values of the various observable quantities. We have, therefore, accordingly skipped the presentation of these results. An important feature of the observed E_2^+ systematics is that it shows a sharp decrease as we move from ^{100}Mo to ^{102}Mo, therefore the E_2^+ state shows a slow decrease till ^{106}Mo. As we pass from ^{106}Mo to ^{108}Mo the E_2^+ shows an increase in its value. We have also presented the values of E_2^+ energy obtained by employing VQP and VQPOH in columns 3 and 4, respectively. It may be noted that the calculated results for E_2^+ obtained with VQPOH are in better agreement with experiments. They reproduced the observed systematics of E_2^+ more closely than the results obtained with VQP. For example the sharp decrease in E_2^+ as we move from ^{100}Mo to ^{102}Mo is very well reproduced. Secondly, the observed increase in E_2^+ energy value as we pass on from ^{106}Mo to ^{108}Mo is also reproduced. However, the results obtained with VQP do not reproduce this increase. In that sense the results obtained with VQPOH interaction are found to be in better agreement with the experiments. Now coming to the discussion

Table 1. The experimental values of excitation energy of the E_2^+ state in MeV (ΔE) and intrinsic quadrupole moments of the HB states in $^{100-110}$Mo isotopes with the VQP and VQPOH interaction. Here $\langle Q_0^2\rangle_\pi$ gives the contribution of the protons to the total intrinsic quadrupole moments. The quadrupole moments have been computed in units of b^2, where $b = \sqrt{\hbar/m\omega}$ is the oscillator parameter.

		Interaction					
Mo		VQP			VQPOH		
Nuclei (A)	E_2^+ (Exp.)	$\langle Q_0^2\rangle_{\rm HB}$	$\langle Q_0^2\rangle_\pi$	E_2^+	$\langle Q_0^2\rangle_{\rm HB}$	$\langle Q_0^2\rangle_\pi$	E_2^+
100	0.53	57.70	20.99	0.27	52.30	20.01	0.40
102	0.29	61.30	20.84	0.24	60.30	20.00	0.29
104	0.19	63.80	21.06	0.22	65.74	21.71	0.17
106	0.17	65.10	31.30	0.20	68.42	22.39	0.14
108	0.19	66.78	21.22	0.16	67.41	22.29	0.17
110	–	63.49	21.22	0.10	66.15	22.10	0.21

of intrinsic quadrupole moments, it is noteworthy that the systematics of $\langle Q_0^2\rangle_{\rm HB}$ obtained with VQPOH interaction are in better agreement with the systematics of observed E_2^+ state. It is well-known that a nucleus having smaller energy gap ΔE should have a larger quadrupole moment for the 2_1^+ state. Since Q_2^+ of the nucleus is directly related to its intrinsic quadrupole moment, one should, therefore, expect that a smaller energy gap ΔE should manifest itself in terms of a larger quadrupole moment and vice-versa. In other words, the observed systematics of E_2^+ with mass number A should produce a corresponding inverse systematics of intrinsic quadrupole moment of Mo nuclei with A. Based on the above logic, the calculated values of intrinsic quadrupole moments should exhibit an increasing trend as one moves from ^{100}Mo to ^{106}Mo and then decrease for ^{108}Mo. It is noted from table 1, that this trend is certainly shown by $\langle Q_0^2\rangle_{\rm HB}$ values obtained with VQPOH. For example the intrinsic $\langle Q_0^2\rangle_{\rm HB}$ increases sharply from 52.30 units to 60.30 units as we go from ^{100}Mo to ^{102}Mo. Further, the $\langle Q_0^2\rangle_{\rm HB}$ values show a decrease as we pass on from ^{106}Mo to ^{108}Mo. The results obtained with VQP show a marginal increase from 65.10 units to 66.78 units which is not observed experimentally. Thus, it can be said that the results on E_2^+ systematics and intrinsic quadrupole moments obtained with VQPOH interaction are in better agreement with experiments than the ones obtained with VQP interaction.

We next focus our attention on the factors that are responsible for making these isotopes to exhibit such features. In tables 2–5 the results of occupation probabilities of valence orbits for protons and neutrons are presented. It is noted from tables 2 and 4 that $\langle Q_0^2\rangle_\pi$ is very sensitively dependent on the occupation of $(g_{9/2})_\pi$ orbit. The values of $\langle Q_0^2\rangle_\pi$, obtained with VQPOH interaction, are less than those obtained with VQP interaction for $^{100-102}$Mo, because of smaller occupation of $(g_{9/2})_\pi$ orbits. A comparison of the results

Table 2. The sub-shell occupation numbers (protons) in $^{100-110}$Mo nuclei with VQP interaction. Here $\langle Q_0^2\rangle_\pi$ gives the contribution of protons to the total intrinsic quadrupole moments.

Mo Nuclei (A)	J^π	Sub-shell occupation number							
		$2s_{1/2}$	$1p_{1/2}$	$1d_{3/2}$	$1d_{5/2}$	$0g_{7/2}$	$0g_{9/2}$	$1h_{11/2}$	$\langle Q_0^2\rangle_\pi$
100	$0^+ \to 6^+$	0.08	0.00	0.04	0.79	0.03	3.03	0.00	20.99
	8^+	0.10	0.00	0.05	0.84	0.04	2.95	0.00	21.27
	$10^+ \to 16^+$	0.11	0.00	0.06	0.89	0.04	2.87	0.00	21.58
102	$0^+ \to 4^+$	0.09	0.00	0.05	0.81	0.03	3.00	0.00	20.84
	6^+	0.09	0.00	0.06	0.85	0.03	2.94	0.00	20.98
	$8^+ \to 16^+$	0.11	0.00	0.08	1.03	0.04	2.62	0.00	23.54
104	$0^+ \to 4^+$	0.11	0.00	0.06	0.85	0.04	2.94	0.00	21.06
	$6^+ \to 10^+$	0.11	0.00	0.06	0.90	0.05	2.85	0.00	22.00
	$12^+ \to 16^+$	0.13	0.00	0.08	0.98	0.06	2.72	0.00	23.42
106	$0^+ \to 6^+$	0.11	0.00	0.06	0.87	0.04	2.91	0.00	21.30
	$8^+ \to 16^+$	0.12	0.00	0.07	1.05	0.05	2.57	0.00	25.42
108	$0^+ \to 8^+$	0.11	0.00	0.06	0.86	0.04	2.91	0.00	21.12
	$10^+ \to 16^+$	0.15	0.00	0.09	0.98	0.06	2.69	0.00	21.60
110	$0^+ \to 16^+$	0.11	0.00	0.06	0.87	0.04	2.89	0.00	21.22

Table 3. The sub-shell occupation numbers (neutrons) in $^{100-110}$Mo nuclei with VQP interaction. Here $\langle Q_0^2 \rangle_\nu$ gives the contribution of neutrons to the total intrinsic quadrupole moments.

Mo Nuclei (A)	J^π	Sub-shell occupation number							$\langle Q_0^2 \rangle_\nu$
		$2s_{1/2}$	$1p_{1/2}$	$1d_{3/2}$	$1d_{5/2}$	$0g_{7/2}$	$0g_{9/2}$	$1h_{11/2}$	
100	$0^+ \rightarrow 6^+$	0.66	1.99	1.31	2.71	1.47	9.78	1.88	36.71
	8^+	0.68	1.99	1.34	2.69	1.56	9.75	1.95	37.73
	$10^+ \rightarrow 16^+$	0.70	1.99	1.36	2.61	1.64	9.72	2.00	38.52
102	$0^+ \rightarrow 4^+$	0.71	1.99	1.38	2.96	1.85	9.80	3.21	40.46
	6^+	0.71	1.99	1.38	2.86	1.84	9.78	3.36	41.52
	$8^+ \rightarrow 16^+$	0.72	1.99	1.38	2.32	1.80	9.67	3.98	44.16
104	$0^+ \rightarrow 4^+$	0.73	1.99	1.40	3.25	2.50	9.81	4.28	42.74
	$6^+ \rightarrow 10^+$	0.73	1.99	1.42	3.16	2.49	9.78	4.40	43.30
	$12^+ \rightarrow 16^+$	0.71	1.99	1.43	2.99	2.50	9.74	4.65	43.88
106	$0^+ \rightarrow 6^+$	0.88	1.99	1.52	3.65	3.01	9.83	5.09	43.80
	$8^+ \rightarrow 16^+$	0.74	1.99	1.41	3.25	2.79	9.75	5.98	45.38
108	$0^+ \rightarrow 8^+$	1.03	1.99	1.65	4.09	3.49	9.87	5.84	45.66
	$10^+ \rightarrow 16^+$	1.08	1.99	1.79	4.39	4.50	9.92	6.30	45.69
110	$0^+ \rightarrow 16^+$	1.13	1.99	1.74	4.61	4.10	9.92	6.48	42.27

Table 4. The sub-shell occupation numbers (protons) in $^{100-110}$Mo nuclei with VQPOH interaction. Here $\langle Q_0^2 \rangle_\pi$ gives the contribution of protons to the total intrinsic quadrupole moments.

Mo Nuclei (A)	J^π	Sub-shell occupation number							$\langle Q_0^2 \rangle_\pi$
		$2s_{1/2}$	$1p_{1/2}$	$1d_{3/2}$	$1d_{5/2}$	$0g_{7/2}$	$0g_{9/2}$	$1h_{11/2}$	
100	$0^+ \rightarrow 4^+$	0.63	0.00	0.08	0.76	0.06	2.44	0.00	20.01
	$6^+ \rightarrow 10^+$	0.63	0.00	0.08	0.75	0.06	2.46	0.00	19.93
	12^+	0.64	0.00	0.09	0.78	0.06	2.40	0.00	20.23
	$14^+ \rightarrow 16^+$	0.64	0.00	0.09	0.80	0.07	2.38	0.00	20.32
102	$0^+ \rightarrow 8^+$	0.66	0.00	0.12	0.84	0.08	2.27	0.00	20.00
	$10^+ \rightarrow 16^+$	0.67	0.00	0.12	0.86	0.09	2.23	0.00	20.20
104	$0^+ \rightarrow 6^+$	0.65	0.00	0.10	0.85	0.07	2.32	0.00	21.71
	$8^+ \rightarrow 16^+$	0.65	0.00	0.10	0.86	0.07	2.29	0.00	21.78
106	$0^+ \rightarrow 16^+$	0.67	0.00	0.11	0.97	0.08	2.14	0.00	22.39
108	$0^+ \rightarrow 14^+$	0.66	0.00	0.10	0.99	0.07	2.16	0.00	22.29
	16^+	0.64	0.00	0.08	0.93	0.05	2.28	0.00	21.77
110	$0^+ \rightarrow 16^+$	0.59	0.00	0.04	0.79	0.03	2.52	0.00	22.10

presented on neutron occupations presented in tables 3 and 5 reveals that $(h_{11/2})_\nu$ for ^{100,102}Mo obtained with VQP is greater than that obtained with VQPOH. Because of this the $\langle Q_0^2 \rangle_\nu$ for VQP is greater than that obtained with VQPOH. It is pointed out that these

Table 5. The sub-shell occupation numbers (neutrons) in $^{100-110}$Mo nuclei with VQPOH interaction. Here $\langle Q_0^2\rangle_\nu$ gives the contribution of neutrons to the total intrinsic quadrupole moments.

Mo Nuclei (A)	J^π	Sub-shell occupation number							$\langle Q_0^2\rangle_\nu$
		$2s_{1/2}$	$1p_{1/2}$	$1d_{3/2}$	$1d_{5/2}$	$0g_{7/2}$	$0g_{9/2}$	$1h_{11/2}$	
100	$0^+ \to 4^+$	1.20	1.99	1.18	2.70	1.59	9.85	1.44	32.29
	$6^+ \to 10^+$	1.20	1.99	1.18	2.74	1.58	9.86	1.41	32.14
	12^+	1.21	1.99	1.19	2.64	1.63	9.84	1.46	32.70
	$14^+ \to 16^+$	1.22	1.99	1.20	2.61	1.65	9.83	1.46	32.86
102	$0^+ \to 8^+$	1.21	1.99	1.19	2.85	1.84	9.86	3.03	40.30
	$10^+ \to 16^+$	1.21	1.99	1.20	2.77	1.86	9.85	3.08	40.84
104	$0^+ \to 6^+$	1.29	1.99	1.30	2.58	2.42	9.84	4.55	44.03
	$8^+ \to 16^+$	1.28	1.99	1.30	2.58	2.42	9.83	4.61	44.24
106	$0^+ \to 16^+$	1.13	1.99	1.42	3.00	2.94	9.79	5.69	46.03
108	$0^+ \to 14^+$	0.96	1.99	1.64	3.83	3.58	9.83	6.13	45.11
	16^+	1.02	1.99	1.62	4.04	3.52	9.86	5.91	43.29
110	$0^+ \to 16^+$	1.17	1.99	1.68	4.92	3.92	9.93	6.35	44.05

occupations are less than half and therefore $k = 1/2$ and 3/2 components of $(h_{11/2})_\nu$ orbit are getting occupied. Their occupation therefore make positive contribution to the intrinsic quadrupole moment as they are down sloping orbits. In ^{104,106}Mo, the $(h_{11/2})_\nu$ occupations with VQPOH are larger than those with VQP and hence the $\langle Q_0^2\rangle_\nu$ components obtained with VQPOH is larger than that obtained with VQP. Further, in ^{108}Mo the $(h_{11/2})_\nu$ occupation becomes more than half with VQPOH and hence the $\langle Q_0^2\rangle_\nu$ shows a decrease which is in agreement with the observed systematics of E_2^+. Thus, the occupation numbers of $(g_{9/2})_\pi$ and $(h_{11/2})_\nu$ orbits obtained with VQPOH interaction determine the deformation systematics in $^{100-108}$Mo.

4. Yrast spectra

In order to determine the efficiency of the VQP and VQPOH models of two-body interaction, a projection calculation for the energy spectra of $^{100-108}$Mo was carried out. In figures 1 and 2, the yrast spectra for $^{100-108}$Mo isotopes is displayed, where we have compared the experimental values of yrast states with the theoretical values (Th. 1 and Th. 2). The spectra corresponding to Th. 1 has been obtained by using VQP two-body interaction whereas the spectra corresponding to Th. 2 has been obtained by including a higher-order octupole–octupole plus hexadecapole–hexadecapole interaction energy term also in the two-body residual interaction (VQPOH). It turns out from our calculations that calculated spectra corresponding to Th. 2 reproduces the observed yrast spectra for $^{100-108}$Mo reasonably well as compared to the yrast spectra corresponding to Th. 1. This level of agreement can be considered to be satisfactory because of a number of considerations. First, the calculation of yrast spectra is a complex many-body calculation involving a minimum of 24 valence particles for ^{100}Mo and a maximum of 32 valence particles for ^{108}Mo. Another

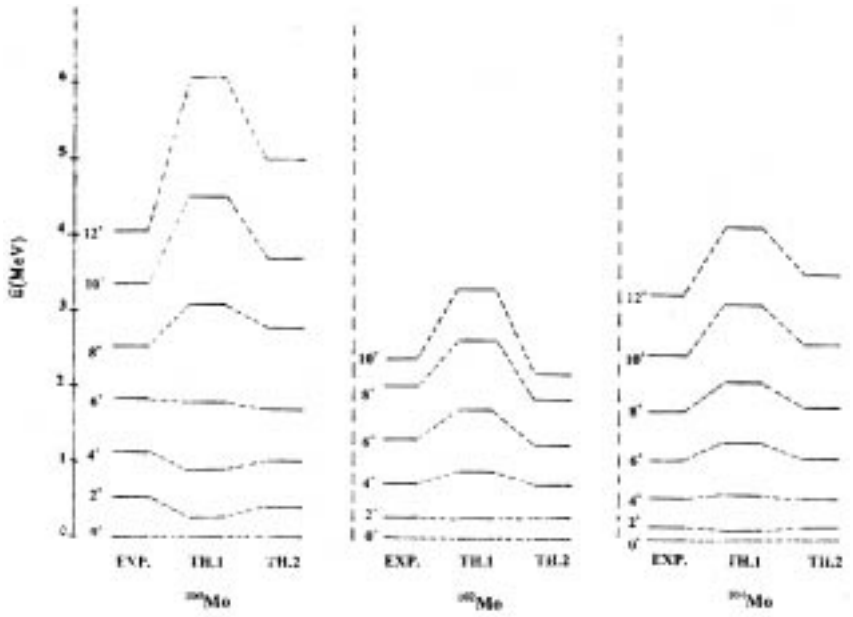

Figure 1. Experimental and theoretical low-lying yrast spectra for $^{100-104}$Mo nuclei (data taken from [22,26,36]).

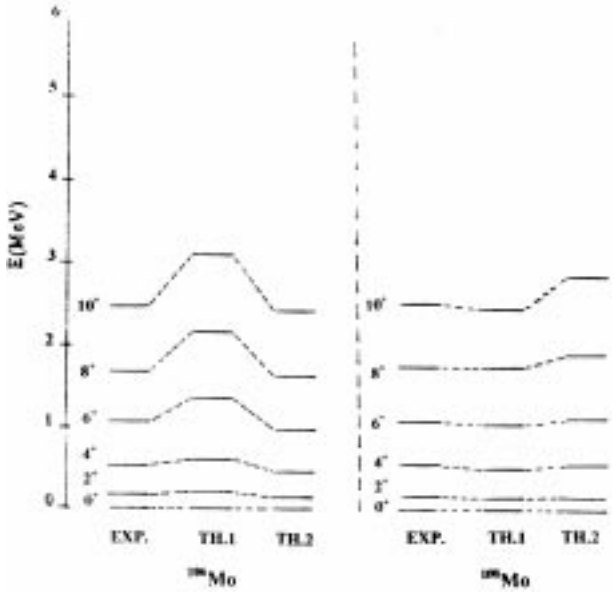

Figure 2. Experimental and theoretical low-lying yrast spectra for $^{106-108}$Mo nuclei (data taken from [22] and [37]).

noticeable fact is that the calculations are carried out for the entire set of the $^{100-108}$Mo isotopes, with a single set of input parameters. Thus, from the figures, it is clear that the inclusion of the hexadecapole–hexadecapole interaction improves the agreement of the calculated spectra with the experiments. We have checked that there is very little difference occurring in the yrast spectra when octupole–octupole interaction term is added to VQP interaction. It was observed by us that inclusion of only octupole–octupole component of two-body residual interaction did not make any noticeable difference to the calculated nuclear structure quantities.

5. Transition probabilities

The reliability and goodness of the HB wavefunction is examined by calculating the $B(E2;0_1^+ \to 2_1^+)$ values. Sometime back Bhatt *et al* [31,32] have developed a formula for the calculation of $B(E2;0_1^+ \to 2_1^+)$ transition probabilities from the values of intrinsic quadrupole moments of protons and neutrons. It has been justified by them that the $B(E2;0_1^+ \to 2_1^+)$ in units of e^2b^2 are given by

$$B(E2;0_1^+ \to 2_1^+) = (1.02 \times 10^{-5})A^{2/3}c^2_{\text{model}}[e_\pi \langle Q_0^2\rangle_\pi + e_\nu \langle Q_0^2\rangle_\nu]^2 \tag{4}$$

where $\langle Q_0^2\rangle_\pi (\langle Q_0^2\rangle_\nu)$ are the intrinsic quadrupole moments of valence protons (neutrons) and e_π and e_ν are the effective charges of the protons and neutrons, respectively. Effective charges of the protons and neutrons are 1.65 and 0.65, respectively for $^{100-108}$Mo. They have recommended the $c_{\text{model}} = (1.11 \pm 0.27)$ for $28 \leq Z \leq 50$ [30]. We have used this formula for the calculation of the $B(E2)$ values for the mass chain of $^{100-108}$Mo isotopes.

In table 6, we present a comparison of the calculated $B(E2)$ values obtained with VQP and VQPOH interaction with the experimental values for the $0_1^+ \to 2_1^+$ transition in case of $^{100-108}$Mo. It is satisfactory to note that the calculated $B(E2)$ values obtained with VQPOH interaction are in satisfactory agreement with the experimental values for the $0_1^+ \to 2_1^+$ transitions in case of $^{102-108}$Mo. In case of ^{100}Mo the calculated value is slightly larger than the observed value. Since the calculations for the $B(E2)$ values depend on the

Table 6. Comparison of the calculated and experimental $B(E2;0_1^+ \to 2_1^+)$ values in $^{100-110}$Mo isotopes. The $B(E2)$ values are in units of $e^2 \cdot b^2$.

Mo Nuclei	$B(E2;0_1^+ \to 2_1^+)$		
(A)	VQP	VQPOH	Expt.
100	1.00	0.85	0.51(10)*
102	1.08	1.04	1.06(12)*
104	1.17	1.25	1.32(9)**
106	1.23	1.36	1.30(7)*
108	1.28	1.35	1.34(31)*
110	1.21	1.32	–

*Data taken from [34].

**Data taken from [35].

intrinsic quadrupole moments, $B(E2)$ values should follow the same trend as that followed by the intrinsic quadrupole moments. This feature of the molybdenum isotopes has been reproduced by the present calculations. Based on the calculated results on $B(E2)$ values, it seems as if the wavefunctions obtained with VQPOH are quite reliable for $^{100-108}$Mo.

6. Back-bending phenomenon

In tables 7 and 8, the experimental as well as theoretical values of moment of inertia (I) vs. square of the cranking frequency (ω^2), obtained with VQP and VQPOH interactions are presented for ^{100}Mo and ^{102}Mo nuclei. These quantities have been computed in terms of the yrast energies by using the following expressions [24]:

$$\frac{2I}{\hbar^2} = \frac{(4J-2)}{E_J - E_{J-2}} \tag{5}$$

and

$$(\hbar\omega)^2 = \frac{[(J^2-J+1)(E_J - E_{J-2})^2]}{(2J-1)^2}. \tag{6}$$

Table 7. Comparison of experimental and calculated values of the moment of inertia (I) and the square of cranking frequency (ω^2) in ^{100}Mo isotope using VQP and VQPOH interactions.

	$2I/\hbar^2$			$\hbar^2\omega^2$		
J^π	Expt.	VQP	VQPOH	Expt.	VQP	VQPOH
2^+	11.32	24.00	15.00	0.093	0.020	0.053
4^+	23.33	21.53	23.33	0.095	0.112	0.095
6^+	30.98	24.44	31.88	0.129	0.207	0.121
8^+	44.11	23.07	27.77	0.117	0.428	0.295
10^+	45.23	27.14	40.86	0.177	0.494	0.218
12^+	65.71	29.67	35.38	0.123	0.604	0.424
14^+	66.66	32.72	34.61	0.164	0.683	0.610

Table 8. Comparison of experimental and calculated values of the moment of inertia (I) and the square of cranking frequency (ω^2) in ^{102}Mo isotope using VQP and VQPOH interactions.

	$2I/\hbar^2$			$\hbar^2\omega^2$		
J^π	Expt.	VQP	VQPOH	Expt.	VQP	VQPOH
2^+	20.68	22.22	20.68	0.028	0.024	0.028
4^+	31.11	22.22	31.81	0.053	0.105	0.051
6^+	37.93	27.16	41.50	0.086	0.168	0.071
8^+	43.47	31.91	51.72	0.120	0.223	0.085
10^+	95.00	59.37	115.1	0.040	0.103	0.027
12^+		56.79	153.3		0.164	0.022
14^+		54.00	125.5		0.251	0.046

Table 9. Quadrupole of deformation parameters (β_2) and hexadecapole deformation parameters (β_4) of the HB states in $^{100-110}$Mo isotopes with the VQP and VQPOH interaction respectively. The experimental β_2 values are taken from [34]. In column 7 the β_4 values are taken from [27].

Mo	VQP		VQPOH		(β_2)	(β_4)
Nuclei	β_2	β_4	β_2	β_4	Expt.	[27]
100	0.24	0.021	0.22	0.027	0.23(22)	0.023
102	0.32	0.022	0.32	0.031	0.32(19)	0.050
104	0.338	0.018	0.34	0.024	0.32(12)	0.030
106	0.339	0.014	0.36	0.017	0.35(10)	−0.002
108	0.344	0.095	0.35	0.010	0.35(41)	−0.027
110	0.33	0.004	0.34	0.002	–	−0.063

The calculated results obtained with VQP interaction predicts back-bending around spins 8^+ in ^{102}Mo, whereas the results obtained with the VQPOH interaction expects back-bending to occur at spin 8^+ in ^{100,102}Mo. Experimentally, back-bending is observed at 10^+ and 8^+ in ^{100}Mo and ^{102}Mo, respectively. This means that with the VQPOH interaction, calculated results are in better agreement with the experiments than with the VQP interaction.

7. Quadrupole (β_2) and hexadecapole (β_4) deformations

In table 9, the calculated values for deformation parameter (β_2 and β_4) have also been presented. The deformation parameter β_2 is related to $B(E2)\uparrow$ by the formula suggested by Raman *et al* [33].

$$\beta_2 = (4\pi/3ZR_0^2)[B(E2)\uparrow/e^2]^{1/2} \tag{7}$$

where R_0 is usually taken to be $1.2A^{1/3}$ fm and $B(E2)\uparrow$ is in units of e^2b^2. In order to check the reliability of the hexadecapole strength parameters and the corresponding HB wavefunction, β_4 have been calculated.

From the systematics of the calculated β_2 and β_4 values, it is noted that the set of values obtained with VQPOH interaction are in satisfactory overall agreement with the observed values.

8. Conclusions

From the results of our calculations, the following conclusions can be drawn:

(1) The VAP calculations performed with VQPOH interaction reproduces correctly the deformation systematics in $^{100-108}$Mo isotopes. The deformation systematics are found to depend sensitively on the occupation probabilities of $(g_{9/2})_\pi$ and $(h_{11/2})_\nu$ orbits.

(2) The results of VAP calculations show a marked improvement in agreement with experiments when hexadecapole interactions are included in the two-body interaction. It seems that the two-body effective residual interaction in Mo isotopes apart from having a dominantly quadrupole character has a finite but small hexadecapole contribution which results in the generation of more accurate intrinsic wavefunction that simulates the observed properties of Mo isotopes better than when only VQP interaction is employed.

(3) The recently observed back-bending in ^{100}Mo is also reproduced by our VAP calculations performed with VQPOH interaction.

(4) The hexadecapole interaction parameter employed by us produces more accurate HB wavefunction which yields values of $B(E2)$ and β_2 in satisfactory agreement with experiments. Besides this the values β_4 for $^{100-104}$Mo are in satisfactory agreement with those predicted by Möller *et al* [27].

(5) The quadrupole–quadrupole plus pairing model of interaction with the inclusion of hexadecapole interaction gives a better overall understanding of properties of $^{100-108}$Mo isotopes.

References

[1] E Cheifetz, R C Jarad, S G Thompson and J B Wilhelmy, *Phys. Rev. Lett.* **25**, 38 (1970)

[2] P Federman and S Pittel, *Phys. Rev.* **C20**, 820 (1979)

[3] J Dobaczewski, in: *Contemporary topics in nuclear structure physics* edited by R F Casten, A Frank, M Moshinsky and S Pittel (World Scientific, Singapore, 1988) p. 227

[4] J L Wood, K Heyde, W Nararewicz, M Huyse and P Van Duppen, *Phys. Reports* **215**, 101 (1992)

[5] P Federman, S Pittel and R Campos, *Phys. Lett.* **B82**, 9 (1979)

[6] W Nazarewicz and T Werner, in: *Nuclear structure of the zirconium region* edited by J Eberth, R A Meyer and K Sistemich (Springer-Verlag, Berlin, 1988) p. 277

[7] W Nazarewicz, in: *Contemporary topics in nuclear structure physics* edited by R F Casten, A Frank, M Moshinsky and S Pittel (World Scientific, Singapore, 1988) p. 467

[8] J P Maharana, Y K Gambir, J A Sheikh and P Ring, *Phys. Rev.* **C46**, R1163 (1992)

[9] S K Patra and C R Praharaj, *Phys. Rev.* **C47**, 2978 (1993)

[10] P Bonche, H Flocard, P H Heenen, S J Krieger and M S Weiss, *Nucl. Phys.* **A443**, 39 (1985)

[11] D A Arseniev, A Sobiczeuski and V V Soloviev, *Nucl. Phys.* **A139**, 269 (1969)

[12] R K Sheline, I Ragnarsson and S G Nilsson, *Phys. Lett.* **B41**, 115 (1972)

[13] A Faessler, J E Golonska, U Gotz and H C Pauli, *Nucl. Phys.* **A230**, 302 (1974)

[14] R E Azuma, G L Borchert, L C Carraz, P G Hansen, B Jonson, S Mattsson, O B Nielsen, G Nyman, I Ragnarsson and H L Ravn, *Phys. Lett.* **B86**, 5 (1979)

[15] X Campi and M Epherre, *Phys. Rev.* **C22**, 2605 (1980)

[16] R Bengtsson, P Moller, J R Nix and J-y Zhang, *Phys. Scripta* **29**, 402 (1984)

[17] I Ragnarsson and R K Sheline, *Phys. Scripta* **29**, 385 (1984)

[18] K Heyde, J Moreau and M Waroquier, *Phys. Rev.* **C29**, 1859 (1984)

[19] D Galeriu, D Bucurescu and M J Ivascu, *J. Phys.* **G12**, 329 (1986)

[20] M Sugita and A Arima, *Nucl. Phys.* **A515**, 77 (1990)

[21] E Kirchuk, P Federman and S Pittel, *Phys. Rev.* **C47**, 567 (1993)

[22] A Guessous, N Schulz, M Bentalab, E Lubkiewicz, J L Durell, C J Pearson, W R Phillips, J A Shannon, W Uaban, B J Varley, I Ahmad, C J Lister, L R Morss, R L Nash, C W Williams and S Khazrouni, *Phys. Rev.* **C53**, 1191 (1996)

[23] S K Sharma, P N Tripathi and S K Khosa, *Phys. Rev.* **C38**, 2935 (1988)
[24] P N Tripathi, S K Sharma and S K Khosa, *Phys. Rev.* **C29**, 1951 (1984)
[25] S K Khosa, P N Tripathi and S K Sharma, *Phys. Lett.* **B119**, 257 (1982)
[26] P H Regan, T M Menezes, C J Pearson, W Gelletly, C S Purry, P M Walker, S Juutinen, R Julin, K Helariutta, A Savelius, P Jones, P Jamsen, M Muikku, P A Butler, G Jones and P Greenlees, *Phys. Rev.* **C55**, 2305 (1997)
[27] P Möller, J R Nix, W D Myers and W J Swiatecki, *At. Data Nucl. Data Tables* **59**, 379 (1995)
[28] A Bohr and B R Mottelson, *Nuclear structure* (New York, Benjamin, 1975) Vol. II, p. 356
[29] S K Sharma, *Nucl. Phys.* **A260**, 226 (1976)
[30] N Onishi and S Yoshida, *Nucl. Phys.* **80**, 367 (1966)
[31] K H Bhatt, C W Nestor Jr and S Raman, *Phys. Rev.* **C46**, 164 (1992)
[32] S Raman, C W Nestor, S Kahane and K H Bhatt, *At. Data Nucl. Data Tables* **42**, 1 (1989)
[33] S Raman, J A Sheikh and K H Bhatt, *Phys. Rev.* **C52**, 1380 (1995)
[34] S Raman, C H Malarkey, W T Milner, C W Nestor Jr and P H Stelson, *At Data Nucl. Data Tables* **36**, 23 (1987)
[35] M Liang, H Ohm, B de Sutter and K Sistemich, *KFA Annual Report* (1989) p. 42
[36] R Estep, R K Sheline, D J Decman, E A Henry, L G Mann, R A Meyer, W Stoeffl, L E Ussery and J Kentele, *Phys. Rev.* **C39**, 76 (1989)
[37] M A C Hotchkis, J L Durell, J B Fitzgerald, A S Mowbray, W R Phillips, I Ahmad, M P Carpenter, R V F Janssens, T L Khoo, E F Moore, Ph Benet and D Ye, *Nucl. Phys.* **A530**, 111 (1991)